ANL/CHM/CP-98062

STUDIES OF HYDROGEN-INDUCED DEGRADATION PROCESSES IN $Pb(Zr_{1-x}Ti_x)O_3$ (PZT) AND $SrBi_2Ta_2O_9$ (SBT) FERROELECTRIC FILM-BASED CAPACITORS

A. R. Krauss[a], A. Dhote[a,b], O. Auciello[c], J. Im[c], R. Ramesh[b], and S. Aggarwal[b]

[a]Argonne National Laboratory, Materials Science and Chemistry Divison, Argonne, IL 60439
[b]University of Maryland, Department of Materials Science and Nuclear Engineering, College Park, MD 20742
[c]Argonne National Laboratory, Materials Science Division, Argonne, IL 60439

Submitted to

Integrated Ferroelectrics

Proceedings of the 11th International Symposium on Integrated Ferroelectrics, Colorado Springs, CO, March 7-10, 1999

*Work supported by the U.S. Department of Energy, BES-Materials Sciences, under Contract W-31-109-ENG-38, the NSF-MRSEC under Grant # DMR-96-32521, and the NSF/ONR under Contract N00014-89-J-1178.

DISCLAIMER

DISCLAIMER

Portions of this document may be illegible in electronic image products. Images are produced from the best available original document.

Submitted to Integrated Ferroelectrics as part of the proceedings of the 11th International Symposium on Integrated Ferroelectrics, Colorado Springs, CO, March 7-10, 1999

STUDIES OF HYDROGEN-INDUCED DEGRADATION PROCESSES IN $Pb(Zr_{1-x}Ti_x)O_3$ (PZT) And $SrBi_2Ta_2O_9$ (SBT) FERROELECTRIC FILM-BASED CAPACITORS

A. R. KRAUSS[a], A. DHOTE[a,b], O. AUCIELLO[c], J. IM[c], R. RAMESH[b], and S. AGGARWAL[b]

[a]Argonne National Laboratory, Materials Science and Chemistry Divisions, Argonne IL 60439; 60439; [b]University of Maryland, Department of Materials Science and Nuclear Engineering, College Park, MD 20742; [c]Argonne National Laboratory, Materials Science Division, Argonne IL.

The integration of PZT and SBT film-based capacitors with Si integrated circuit technology requires the use of processing steps that may degrade the performance of individual device components. Hydrogen annealing to remove damage in the Si FET adversely affects both PZT and SBT, although the mechanisms of degradation are different. We have used Mass spectroscopy of recoiled ions (MSRI), X-ray diffraction (XRD), Raman spectroscopy and electrical characterization to study the mechanisms of hydrogen-induced degradation in these two materials. The mechanism responsible for degradation in SBT during hydrogen annealing appears to be hydrogen-induced volatilization of Bi from the near-surface region during film growth. Although there is a similar, but smaller, loss of Pb in PZT, the resulting change in stoichiometry is not responsible for the degradation of the ferroelectric properties. Raman spectroscopy reveals that PZT films exposed to hydrogen exhibit evidence for the formation of polar hydroxyl [OH^-] bonds, which can block the movement of ions in the lattice and inhibit polarization. The possible sites for the incorporation of hydrogen are discussed in terms of ionic radii, and crystal structure.

Keywords: BST, PZT, hydrogen annealing, ferroelectric, thin film, surface analysis, ion scattering, pulsed ion beam surface characterization

Work supported by the U. S. Department of Energy, BES-Materials Sciences, under Contract W-31-109-ENG-38, the NSF-MRSEC under Grant # DMR-96-32521, and the NSF/ONR under contract N00014-89-J-1178

INTRODUCTION

Non-volatile ferroelectric random access memory (NVFRAM) devices such as the "Smart Cards" currently being brought into use represent the entering wedge of a new wave of electronic products based on ferroelectric thin film technology. These devices utilize an SBT or PZT ferroelectric capacitor integrated with transistors in CMOS devices. In high density NVFRAMs, the capacitor is fabricated above the transistor and connected to the drain via a polysilicon plug (Fig. 1). An adhesion layer (typically Ti) is then deposited onto the plug,, followed by the bottom electrode (typically Pt) of the capacitor. The ferroelectric layer can be produced by physical vapor deposition, chemical solution metalorganic chemical decomposition (MOD), or metalorganic chemical vapor deposition (MOCVD), including a high temperature annealing step. MOCVD is perhaps the most suitable ferroelectric film synthesis method for NVFRAM fabrication. The capacitor is completed by the deposition of the Pt top electrode. Finally, a high temperature anneal in a hydrogen-containing gas is carried out in order to eliminate dangling bonds at the Si/SiO_2 interface of the CMOS transistor. This annealing process improves the properties of the silicon portion of the device, but results in a degradation of the ferroelectric capacitor performance [1-3]. It has been shown [4], for example, that annealing of PZT capacitors in a forming gas mixture containing 30 mTorr partial pressure of H_2 in N_2 at a temperature of 200-400 °C results in a near-complete suppression of the remanent polarization. On the other hand, annealing of SBT capacitors results in an increase in the leakage current by several orders of magnitude [5].

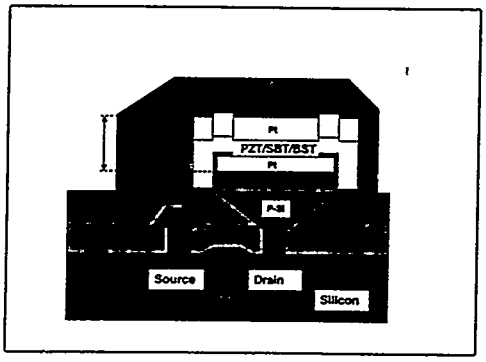

FIGURE 1. Cross section view of a high density (vertically stacked) NVFRAM.

We have studied the composition of the free surface of the ferroelectric film during annealing in hydrogen using *in situ* mass spectroscopy of recoiled ions (MSRI), as well *ex situ* methods including Raman spectroscopy, X-ray diffraction (XRD) and electrical characterization to better understand the mechanism of the degradation process. This understanding also provides guidance in formulating methods to prevent or subsequently correct the degradation of the ferroelectric properties.

Possible mechanisms for the loss of ferroelectric polarization during hydrogen annealing include (1) the loss of lattice oxygen [4], (2) loss of one or more of the cation species [5], and (3) the incorporation of hydrogen into the lattice with subsequent inhibition of polarization. The structures of PZT and SBT (Fig. 2) are quite different. PZT is a pseudo-cubic perovskite with all the Pb atoms in equivalent positions, while SBT is a layered perovskite with a unit cell that is terminated with a bismuth oxide layer consisting of two non-equivalent types of Bi sites. It is not necessarily the case that the same oxygen or cation loss processes occur in the two materials.

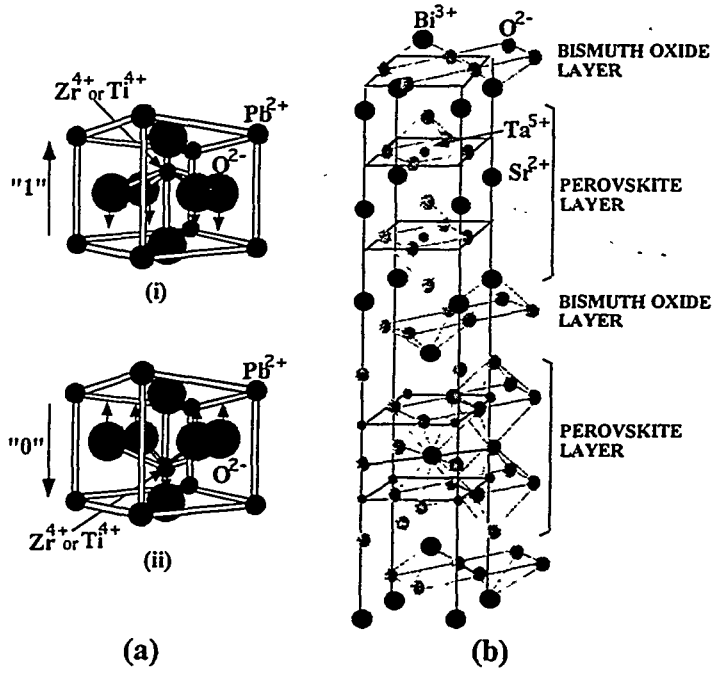

FIGURE 2 The crystal structure of (a) PZT, and (b) SBT

EXPERIMENTAL

The Pt/SBT/Pt capacitors were prepared by sol-gel processing, on a Si substrate with a patterned Pt top electrode. MSRI measurements were made on the areas of exposed ferroelectric between the Pt pads. The PZT films used in the MSRI measurements were prepared by MOCVD deposition on a Pt bottom electrode on an MgO substrate and annealed in air at 650 °C for 30 minutes to form the perovskite phase. The PZT films used for the ex situ measurements were prepared by sol-gel deposition. The substrates were either LSCO/Pt/Si or (for the Raman spectroscopy measurements) LSCO/$LaAlO_3$, where LSCO is a conductive $La_{0.5}Sr_{0.5}CoO_3$ electrode layer. The top electrodes consisted of 100 μm x 100 μm Pt pads.

In situ characterization of the surface composition during film annealing in H_2 was accomplished using a custom-designed time of flight ion scattering and recoil

spectroscopy (TOF-ISARS) system. A schematic of the system is shown in Fig. 3, and a detailed description is presented elsewhere [6,7]. The system is capable of performing simultaneous ion scattering spectroscopy, direct recoil spectroscopy, and MSRI, although only the MSRI capability was used in the present work.

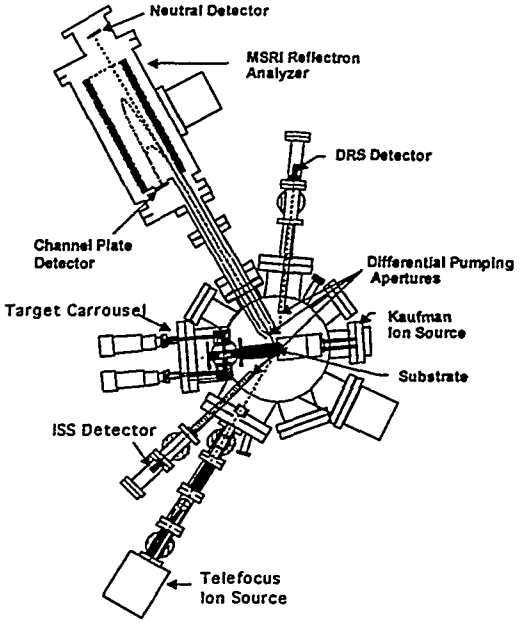

FIGURE 3 Schematic of the TOF-ISARS system indicating the location of the ion beam sputter deposition system, pulsed ion beam line, and ISS, DRS, and MSRI detectors.

The pulsed analysis beam, required for the time-of-flight MSRI method is provided by a telefocus ion source (Atomika W160) in conjunction with a custom-made beam line, including beam focusing lenses, pulsing electrostatic plates, and apertures to produce a pulsed beam with adjustable pulse widths in the range ~ 10-1000 nsec. A final set of dc deflection plates is used to steer the beam to the desired location on the sample. The MSRI analyzer views the sample through a 1 mm diameter aperture at the end of the MSRI extraction optics. By differentially pumping the space behind the apertures, it is possible to maintain a detector vacuum approximately three orders of magnitude lower than that of the sample environment, which can reach pressures in the mTorr range. This scheme provides the unique capability to perform *in situ* studies of film growth and surface and interface phenomena in relatively high pressure environments [6-8].

RESULTS

The ferroelectric hysteresis loop of a Pt/SBT/Pt capacitor is shown in Fig. 4 before hydrogen annealing and after annealing at 500 °C for ten minutes in various partial pressures of hydrogen. At 30 mTorr, the hysteresis loop reveals behavior characteristic of a leaky dielectric, As shown in Fig. 5, the leakage current has increased by 9 orders of magnitude as a result of hydrogen annealing.

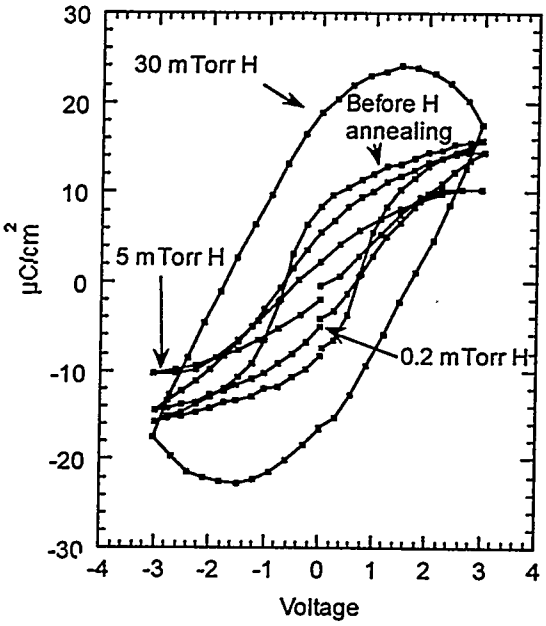

FIGURE 4. Ferroelectric hysteresis loops for a Pt/SBT/Pt capacitor before hydrogen annealing and after annealing at 500 °C for 10 minutes in partial pressures of 0.2 mTorr, 5 mTorr, and 30 mTorr.

Scanning electron microscopy (Fig. 6) shows no change in the SBT film morphology as a result of the hydrogen annealing, and x-ray diffraction (Fig. 7) shows no change in structure or lattice spacing. However, MSRI analysis of the free SBT surface (Fig. 8) shows a pronounced loss of Bi as a result of hydrogen annealing. Fig. 9 represents the MSRI peak intensity as a function of hydrogen partial pressure, showing a marked drop in Bi film content in the near surface region for hydrogen partial pressure in excess of 10 mTorr. Separate measurements involving the deliberate deposition of non-ferroelectric layers greater than 3 nm in thickness are sufficient to destroy the ferroelectric properties of SBT [5]. MSRI is therefore capable of detecting changes that profoundly affect the ferroelectric properties but are not reflected in the bulk properties of the film.

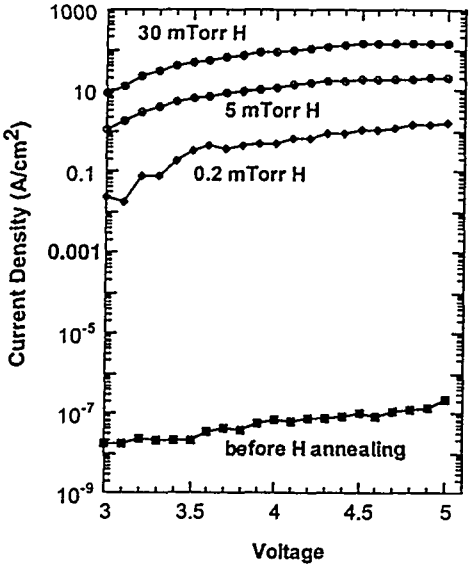

FIGURE 5. Current density-voltage plots for a Pt/SBT/Pt capacitor before hydrogen annealing and after annealing at 500 °C for 10 minutes in partial pressures of 0.2 mTorr, 5 mTorr, and 30 mTorr.

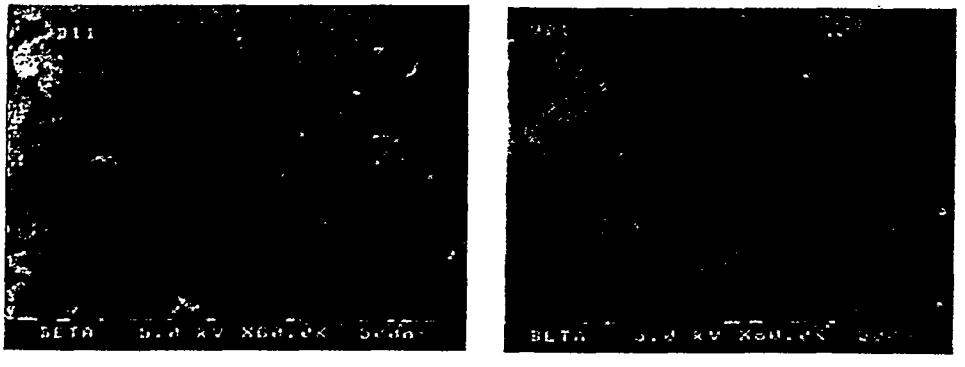

(a) before H anneal (b) after H anneal

FIGURE 6. SEM images of SBT films (a) before and (b) after hydrogen annealing.

The manner in which hydrogen annealing degrades the ferroelectric properties of a Pt/PZt/Pt capacitor is very different from that of Pt/SBT/Pt. As shown in Figure 10, significant degradation in the remanent polarization occurs for forming gas (30 mTorr H_2 partial pressure) annealing temperatures as low as 200 – 300 °C. The decrease in resistivity (Fig. 10 inset) for annealing at 200 °C is less than one order of magnitude. The capacitor structure was formed by patterning the upper electrode prior to the annealing step. The composition of the free PZT surface at the upper electrode as measured by MSRI is shown in Fig. 11 as a function of the annealing temperature. There is a slight drop in Pb concentration at 500 °C, but there is no obvious change in surface composition at 200-300 °C, the temperature range at which remanent polarization disappears. There is a drop in the measured H signal in this range, although the residual hydrogen level appears to stabilize between 300 and 500

°C. This is in marked contrast with the SBT data of Figure 8, in which the incorporated surface hydrogen disappeared after extensive annealing.

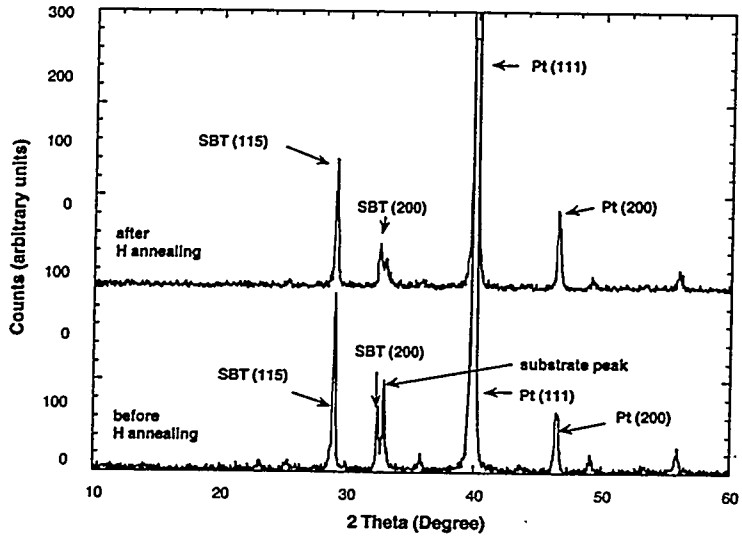

FIGURE 7. X-ray diffraction spectra of SBT films before and after hydrogen annealing.

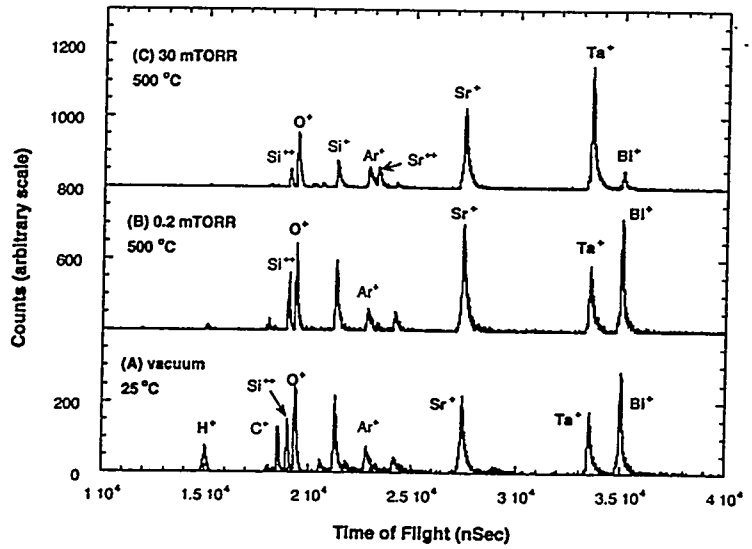

FIGURE 8. MSRI spectra of SBT films before and after hydrogen annealing at 0.2 and 30 mTorr at 500 °C for ten minutes

As shown in the XRD data of Fig. 12, there is no change in the PZT bulk crystalline structure, Figure 13 shows the Raman spectra for epitaxial PZT/LSCO and LSCO layers on an $LaAlO_3$ substrate after a forming gas anneal at 450 °C for 30 minutes. The features in the spectrum are all associated with the PZT film, as evidenced by the complete lack of structure in the spectrum of the LSCO/$LaAlO_3$ layers. The principal peak positions before the forming gas anneal are indicated by the lines in Fig. 13 and correspond to stretching modes of PZT. The primary result of

the annealing is the appearance of the 3650 cm^{-1} OH stretch mode as shown in the inset. The large increase in this signal is taken as evidence of the incorporation of hydrogen into the PZT lattice. However, the lack of bending modes in the Raman spectrum indicate that planar hydrogen positions are unlikely. As discussed by Aggarwal et. al., [4], the 3650 cm-1 peak is consistent with the incorporation of hydrogen in an apical oxygen site, forming an OH molecule that blocks the motion of the Ti^{4+} ion along the (001) polarization direction.

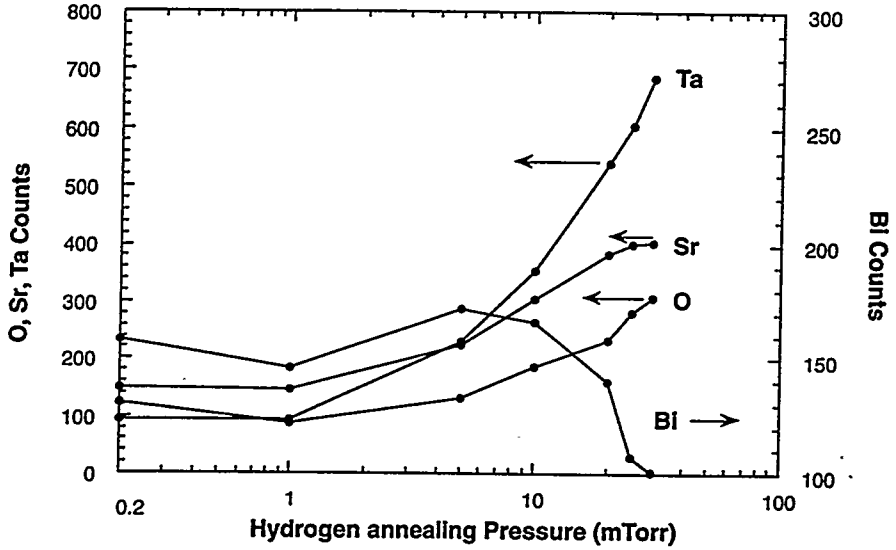

FIGURE 9. Peak intensities of the MSRI spectra of SBT films before and after hydrogen annealing for 10 minutes at 500 °C as a function of hydrogen partial pressure.

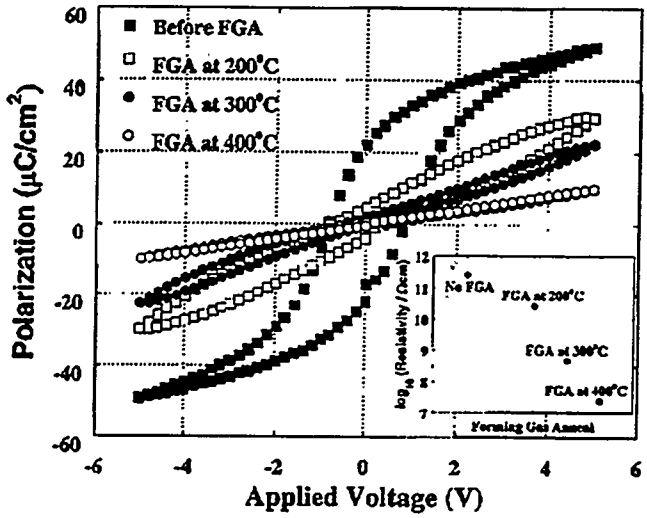

FIGURE 10. Polarization-voltage hysteresis loops for Pt/PZT/Pt capacitors before and after forming gas anneals at temperatures between 200 and 400 °C.

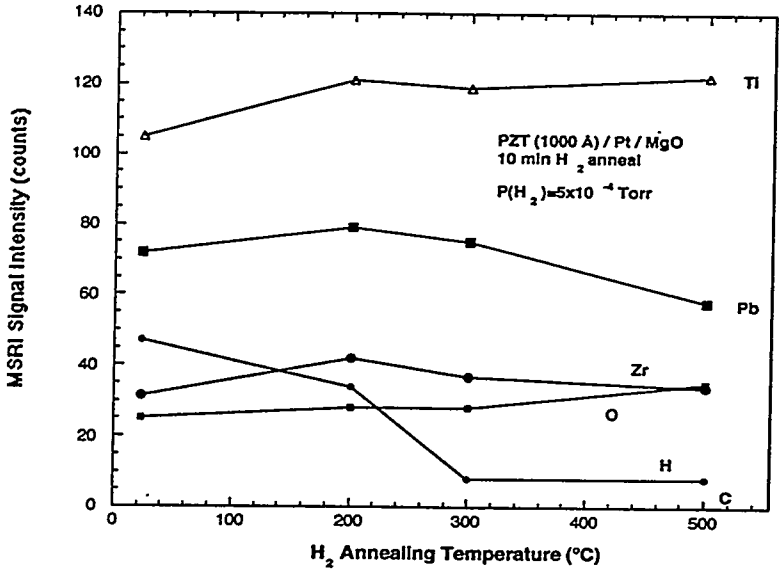

FIGURE 11. Peak intensities of the MSRI spectra of PZT films before and after hydrogen annealing a pressure of $5x10^{-4}$ Torr for 10 minutes at 500 °C as a function of annealing temperature.

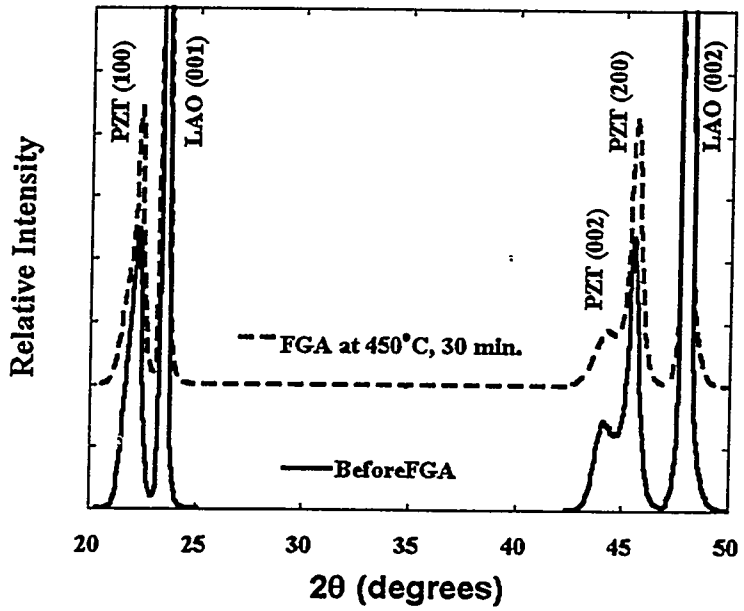

FIGURE 12. X-ray diffraction spectra of PZT films before and after hydrogen annealing at 450 °C at a partial pressure of 30 mTorr for 30 minutes.

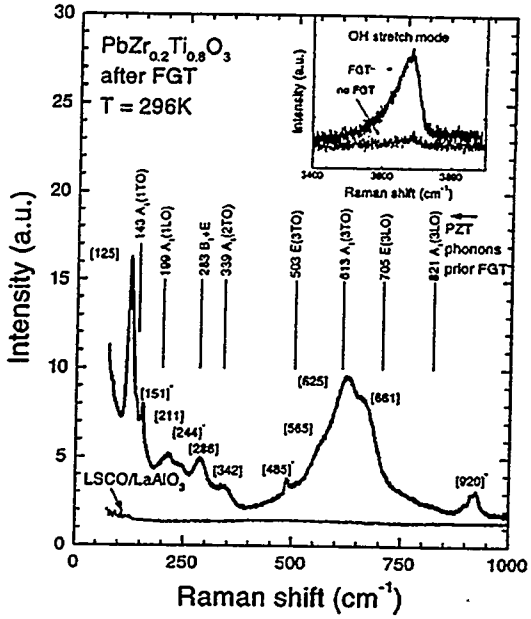

FIGURE 13. Raman spectrum for an epitaxial PZT film deposited on (001) $LaAlO_3$ substrates with a LSCO bottom electrode. The inset shows the region of the 3650 cm^{-1} [OH^-] stretch mode before and after annealing.

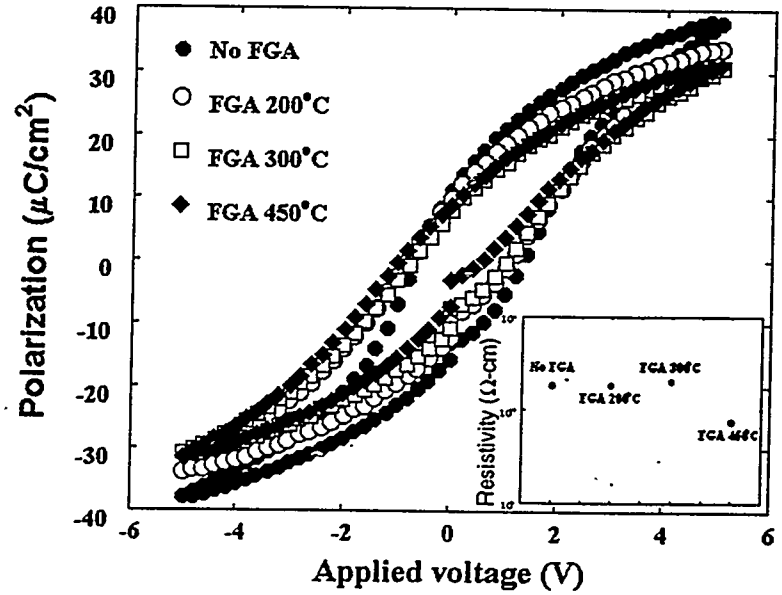

FIGURE 14 Polarization-voltage hysteresis loops for LSCO/PZT/LSCO capacitors before and after forming gas anneals at temperatures of 300 and 450 °C. with continuous LSCO top electrodes.

Pt allows the ready diffusion of hydrogen at elevated temperatures. However, most oxides have limited hydrogen diffusivity. By reversing the order of the top electrode patterning and hydrogen annealing steps (i.e. annealing before patterning), the

LSCO top electrode may be used as a hydrogen permeation barrier. The result is shown in Fig. 14. Little deterioration of the remanent polarization is observed for annealing temperatures up to 450 °C.

CONCLUSIONS

Both PZT and SBT are subject to degradation of the remanent polarization as a result of hydrogen annealing. However, the mechanism is different for the two materials. In the case of SBT, the loss of ferroelectric properties appears to be related to the formation of a thin non-stoichiometric (presumably non-ferroelectric) layer ≥ 3 nm in thickness. For PZT, the mechanism by which remanent polarization is destroyed is associated with neither the loss of stoichiometry nor with change in the lattice structure, but is consistent with inhibition of motion of the Ti ions via formation of an [OH^-] at the apical oxygen sites. However, further work is necessary to confirm these hypotheses.

We would like to thank A. I. Kingon and S. H. Kim for supplying the SBT films.

References

1. Y. Shimamoto, K. Kushida-Abdelghafar, H. Miki, and Y. Fujisaki, Appl. Phys. Lett. **70**, 3096 (1997)
2. K. Kushida-Abdelghafar, H, Miki, K. Torii, and Y. Fujisaki, Appl. Phys. Lett. **69**, 3188 (1996)
3, J.-P. Hahn and T. P. Ma, Appl. Phys. Lett. **71**, 1267 (1997)
4. S. Aggarwal, S. R. Perusse, C. W. Tipton, R. Ramesh, H. D. Drew, T. Venkatesan, D. B. Romero, V. B. Podobedov, and A. Weber, Appl. Phys. Lett. **73**, 1973 (1998).
5. J. Im , O. Auciello, A. R. Krauss, D. M. Gruen, R. P. H. Chang, S. H. Kim and A. I. Kingon, Appl. Phys. Lett. **74**, 1162 (1999)
6. J. Im, A. R. Krauss, Y. Lin, J. A. Schultz, O. Auciello, D. M. Gruen, R. P. H. Chang, Nucl. Instrum. Meth. **B118**, 1996, 772.
7. A. R. Krauss, Y. Lin, O. Auciello, G. J. Lamich, D. M. Gruen, J. A. Schultz, R. P. H. Chang. J. Vac. Sci.Technol. **A12,** 1994, 1943.
8. A. R. Krauss, J. Im, J. A. Schultz, V. S. Smentkowski, K. Waters, C. D. Zuiker, D. M. Gruen, R. P. H. Chang. Thin Solid Films **270**:, 1995, 130.